

Lidar observations of midlatitude stratospheric aerosol layer during long-term volcanically quiet period

V.V. Zuev, V.D. Burlakov, A.V. El'nikov, and A.V. Nevzorov

Institute of Atmospheric Optics, Siberian Branch of the Russian Academy of Sciences, Tomsk

Received November 22, 2005

Under analysis are lidar measurements of optical characteristics of stratospheric aerosol layer, obtained at midlatitude Siberian Lidar Station of the Institute of Atmospheric Optics SB RAS, Tomsk (56.5°N; 85.0°E) under background conditions for long-term volcanically quiet period (VQP) 1996–2005. The results are compared with earlier observations in Tomsk (since 1986) and observations at other midlatitude stations of the Northern Hemisphere. The background aerosol loading of the stratosphere under conditions of long-term VQP is less than for background period 1989–1990. Variations of integrated content and vertical distribution of aerosol in the midlatitude stratosphere are attributed to changes of stratospheric general circulation through influence of meridional transfers from the tropical belt to mid-latitudes, that supports the hypothesis on the presence of tropical reservoir of not only volcanic, but also background stratospheric aerosol.

Introduction

The strongest explosive eruptions of volcanoes El Chichon, Mexico (March–April 1982) and Mt. Pinatubo, Philippines, (June 1991) in XX century have stimulated the development of intensive studies of the stratospheric aerosol layer (SAL) involving remote laser sensing methods. In periods of elevated volcanic aerosol loading of stratosphere, the radiative-temperature effects of the stratospheric aerosol (SA) and its role in heterogeneous stratospheric chemistry manifest themselves most clearly. *In situ* field measurements in this period are most favorable for studies of interrelations between radiative-temperature characteristics of the atmosphere and Earth surface with SA characteristics.

Maximal global mass of sulfuric acid SA after eruption of Mt. Pinatubo was estimated between 21 and 40 Mt, whereas for background periods the estimate ranges from 0.6 to 1.2 Mt.¹ At the same time, the stratospheric aerosol optical depth, considered as the main parameter determining SAL impact on radiation regime of atmosphere and climate effects,² is estimated as 0.004–0.007 at $\lambda = 0.55 \mu\text{m}$ for Northern Hemisphere in background periods; whereas after eruption of Mt. Pinatubo, it reached 0.2 (Refs. 1 and 3). In periods of maximal aerosol loading of stratosphere, the *in situ* measurements detect significant radiative-temperature effects, namely a decrease of near-surface temperature by a few tenths of degree due to scattering of shortwave solar radiation by volcanic aerosol and a few-degree temperature increase at altitudes of the layer localization due to absorption of upward infrared radiation of the Earth.^{4,5}

To study in detail the processes of development and relaxation of aerosol perturbations in stratosphere after powerful volcanic eruptions, tens of existing and newly created observatories and lidar

installations actively operate throughout the globe. Real impetus was given to their uniting into a network of lidar stations aiming at execution of purposeful measurement programs.

In period of stratosphere perturbation by explosive volcanic eruptions, the vertical SAL structure consists of individual layers whose positions depend on stratospheric transport of volcanic aerosols and sulfur-containing gases serving precursors of chemical formation of SA, which, on average, consist of 75% of water-solved sulfuric acid. A long-term, relatively stable SAL structure is formed in background periods under impact of chemical, radiation, and dynamical factors. The main source of background sulfuric acid SA is the emission of natural and anthropogenic sulfur-containing gases from the Earth surface. As recent model calculations show,^{7,8} sulfur dioxide is the main gas precursor of the background SA in addition to carbonyl sulfide (OCS). The OCS contribution to the resulting flux of background SA gaseous precursors from troposphere to stratosphere is somewhat more than 50%, while SO₂ contributes just under 50% (Ref. 8).

By 1996, the stratospheric aerosol of volcanic origin has relaxed, and the level of aerosol stratospheric loading has returned to pre-Pinatubo values; then it became even lower than in background periods of 1979 and 1989–1991. The so-called “new” background period⁶ of SAL state has begun. After 1991, no explosive volcanic eruptions emitting their products immediately to stratosphere were observed. The present-day stratospheric state is characterized by a long-term volcanically quiet period (VQP). This is the longest VQP since stratosphere has come under studies by modern satellite and ground-based observation facilities. After powerful eruption of Agung in 1963, next explosive eruptions up to 1991 were separated in time by less than ten-year periods.³ For instance, optical particle counter

balloon measurements of SA size distribution for 1971–2001 in Laramie, Wyoming (41°N, 105°W), indicate that volcanoes determined aerosol content for 20 years out of 30 years of observations.¹⁸

Studies of SAL state in the absence of volcanic aerosol are also important and are of independent interest. They include: determination of optical characteristics of background SA; study of long-term relaxation trends of volcanic aerosols; ground-based determination of natural and anthropogenic sources of background SA; climatology of background SA; photochemistry and heterogeneous chemistry on the sulfuric acid aerosol surface; detection and study of effects of background SA altitudinal distribution indiscernible under conditions of elevated volcanic aerosol content; study of the processes of stratosphere–troposphere exchange under conditions of clear and stable stratosphere; and study of zonal and meridional SA transport.

The lidar studies of SAL characteristics at the Siberian Lidar Station of the Institute of Atmospheric Optics SB RAS in Tomsk (56.5°N; 85.0°E) are carried out since 1986. The results obtained both in volcanically perturbed and in background periods were considered earlier.^{9–13} Here, we present and analyze the recent results, which reflect SAL state for midlatitudes under conditions of long-term VQP. The integrated SAL characteristics and seasonal variations of vertical SAL structure are considered. The regular sensing of SAL were performed at a unified wavelength of 532 nm; lidar returns were received using a mirror of 0.3-m in diameter and were recorded in the pulse counting mode. Description of the lidar system in more detail is given in Ref. 14.

1. Time behavior of the integrated aerosol backscattering coefficient

Data of laser sensing in the height interval H are used to determine the vertical profile of aerosol backscattering coefficient $\beta_{\pi}^a(H)$. Its values decrease

according to exponential law as the altitude grows. The aerosol stratification can be represented more clearly in terms of the scattering ratio $R(H)$:

$$R(H) = [\beta_{\pi}^a(H) + \beta_{\pi}^m(H)]/\beta_{\pi}^m(H), \quad (1)$$

where $\beta_{\pi}^m(H)$ is molecular backscattering coefficient.

In lidar measurements, the general pattern of time dynamics of aerosol loading can be expressed most adequately through the integrated aerosol backscattering coefficient B_{π}^a in a certain interval of stratospheric heights between h_1 and h_2 :

$$B_{\pi}^a = \int_{h_1}^{h_2} \beta_{\pi}^a(h) dh. \quad (2)$$

The methodical problems of reconstruction of SAL optical characteristics are considered in Ref. 15. The lidar measurement error grows with increasing sensing height because of attenuation of signal from high altitudes. In our measurements, the $R(H)$ measurement error ranges from 3 to 4% in a height interval of 10–20 km; and it increases to 6.5% at an altitude of 30 km. The error of B_{π}^a determination does not exceed 5%.

Figure 1 presents the time behavior of decadelly averaged integrated aerosol backscattering coefficients, which characterize the stratospheric aerosol loading for 1986–2005. For comparison, we also partly present data of analogous lidar measurements at the midlatitude station in Minsk (54°N, 28°E),¹¹ which show analogous time variations of the stratospheric aerosol content. Straight lines show linear regression of B_{π}^a , approximated by the linear fit of the form $B_{\pi}^a = A + Bt$, where A and B are constants; t is the time in decades. For 1986–1991, the formula has the form $B_{\pi}^a = 2.5766 \cdot 10^{-4} - 5.0636 \cdot 10^{-7}t$. For 2000–2005, it changes to $B_{\pi}^a = 1.4788 \cdot 10^{-4} - 1.418 \cdot 10^{-8}t$. The background period

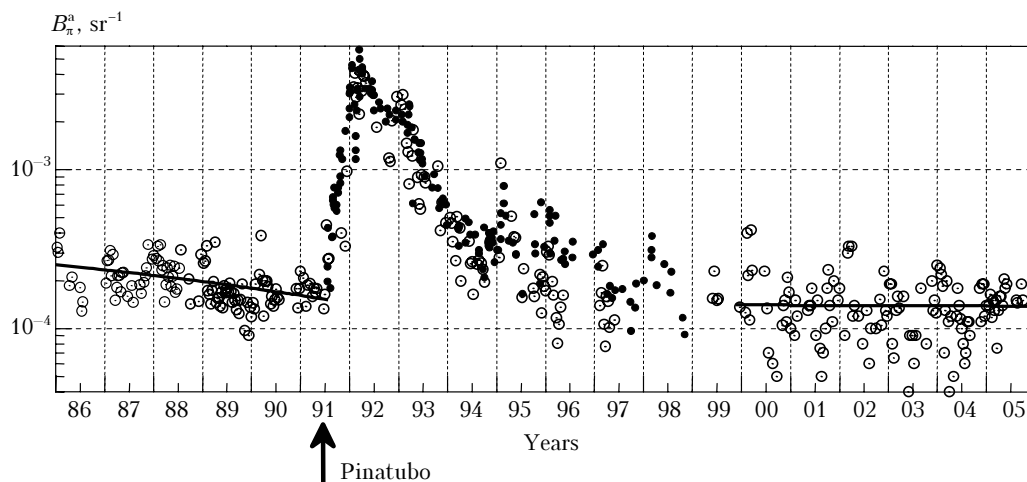


Fig. 1. Time behavior of integrated aerosol backscattering coefficient at $\lambda = 532$ nm over Tomsk within height interval 15–30 km (circles) and Minsk in altitude range 13–30 km (black points); straight lines show the linear regression.

1989–1991 corresponds to a pronounced drop of B_{π}^a for 1986–1991, caused by relaxation of elevated stratospheric aerosol loading after powerful eruptions of El Chichon (1982), del Ruiz (1985), and weaker volcanoes Nyamuragira (1986) and Kelut (1990). In the interval 2000–2005, which corresponds to long-term VQP, a fall of B_{π}^a is not observed and a stable medium-level SA content remains. It has seasonal (winter maximum and summer minimum), quasibiennial,¹⁹ and other variations under impact of dynamical atmospheric factors. The short-term increases of SA content are also possible: during changes of thermodynamical conditions in stratosphere caused by sudden stratospheric warmings²¹ (increased B_{π}^a values in January–March 2000); during formation of polar stratospheric clouds⁹ (increased B_{π}^a values in January 1995); after intense meteor showers,¹² etc.

In 1996, the SA returned to the 1989–1990 level and further became even lower. In 2000–2005, the integrated aerosol backscattering coefficient decreased to its minimum of $5 \cdot 10^{-5} \text{ sr}^{-1}$ versus average values of $(1.5 - 2) \cdot 10^{-4} \text{ sr}^{-1}$ in 1989–1990. Lidar studies in Garmisch-Partenkirchen, Germany (48°N , 11°E)⁶ and Hampton, USA (37°N , 76°W)^{16,17} also have shown currently observed levels of aerosol content in the midlatitude stratosphere to be lower than in volcanically quiet periods 1979 and 1989–1990, which were earlier considered as periods of background content of stratospheric aerosols. Thus, the present-day background levels of SA content turned out to be lower than previously thought. Comparison of SA content in periods 1979, 1989–1990, and after 1996 does not support the existing hypothesis of annual anthropogenic growth of the background level of SA content. The hypothesis of anthropogenic increase of background SA mass up to 5% per year was proposed on the basis of comparison of aerosol content in background periods 1979 and 1989–1990.²⁶ Model calculations suggest that, given 4.5% annual increase of anthropogenic flux of carbonyl sulfide to the stratosphere, by 2050 the SA optical depth will increase by more than an order of magnitude, while the mean near-surface temperature will decrease by 1.5° (Ref. 27). In connection with the problem of possible climatic consequences of anthropogenic increase of SAL depth, studies in this field are of great recent concern.

2. Peculiarities of vertical distribution of background stratospheric aerosol

Observations under conditions of the unperturbed stratosphere make it possible to record effects of aerosol altitude distribution in the stratosphere, earlier indiscernible against the background of increased residual content of volcanic aerosols. Figure 2 shows examples of typical profiles of vertical SA distribution for different seasons in the last years.

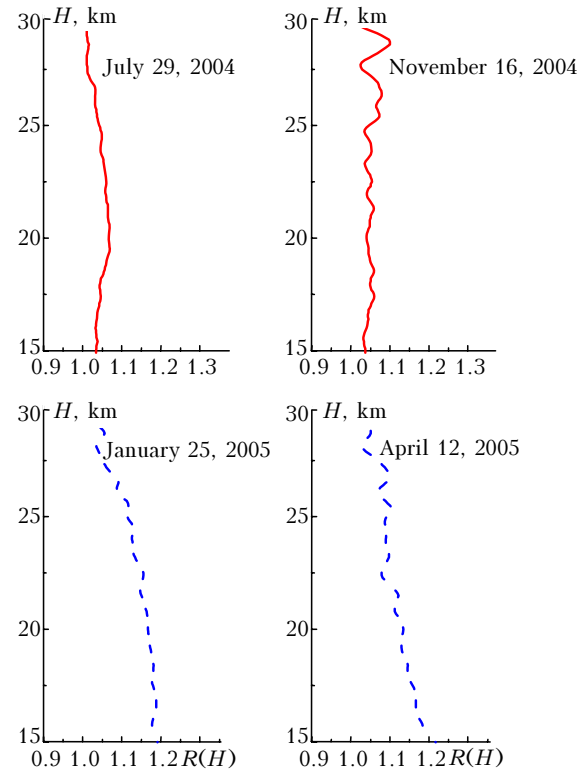


Fig. 2. Examples of typical profiles of vertical distribution of stratospheric aerosol for different seasons.

The summer–fall profiles are mainly characterized by aerosol content uniform in altitude, and minimal scattering ratios $R(H) \sim 1.05\text{--}1.1$. For winter–spring period, there is some increase of aerosol content in the lower stratosphere (up to heights of ~ 20 km) as compared to the summer–fall period, and a growth of $R(H)$ up to 1.15–1.2. This is clearly seen in Fig. 3, which presents the profiles of altitudinal distribution $R(H)$, averaged over half-years, for the measurement period November 2000 – May 2005. For averaging, we used about 60 profiles of summer–fall periods and about 80 profiles of winter–spring periods. At the same time, each individual profile is obtained by averaging of 2–3 measurements for a night. At altitudes below 20 km, $R(H)$ for the winter–spring period still remains higher than for the summer–fall period.

Seasonal variations of stratospheric aerosol loading are most pronounced in periods after explosive eruptions of volcanoes of tropical and subtropical belts. In accordance with models of general stratospheric circulation, in winter–spring period there is observed an increase of meridional stratospheric transport of air masses and aerosol from the tropical reservoir to the middle and high latitudes,²² that is confirmed by midlatitude lidar stations^{9,11,16,17,20} and satellite SAGE measurements.^{22,24,25} The fact that the recorded seasonal differences of aerosol loading of the midlatitude stratosphere hold under conditions of the volcanically unperturbed stratosphere of long-term VQP may indicate that there is a tropical reservoir of not only volcanic but also background SA. Modern

models^{7,8} of stratospheric background sulfuric acid aerosols show that new particles form from sulfur-containing gas precursors of natural and anthropogenic origin predominately in the lower tropical stratosphere. The observed seasonal differences in abundance of midlatitude SA (Fig. 3) also manifest themselves in the lower stratosphere in winter–spring period, when the meridional transport delivers additional aerosol from the tropical reservoir.

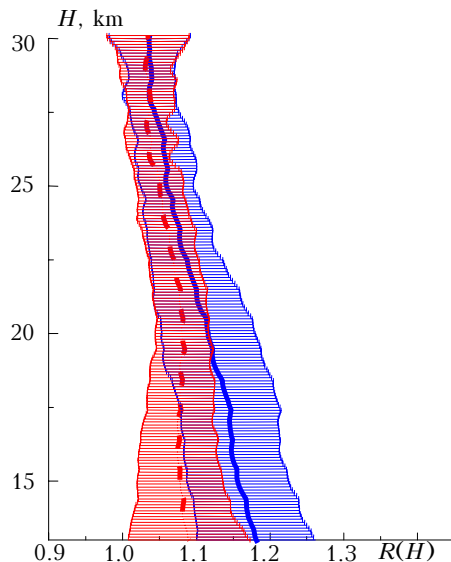


Fig. 3. Seasonally mean profiles of vertical distribution of stratospheric aerosol for period November 2000 – May 2005 (dashed line is for summer–fall and solid line for winter–spring). Thin horizontal lines show standard error corridors.

Based on profiles of 2002–2005 for all seasons, we compiled an average background profile of aerosol backscattering coefficient at $\lambda = 532$ nm for midlatitude stratosphere (Tomsk) under conditions of long-term VQP. This profile is compared in Fig. 4 with the well-known statistical background model,²³ as well as with our model for background period 1989–1990.⁹

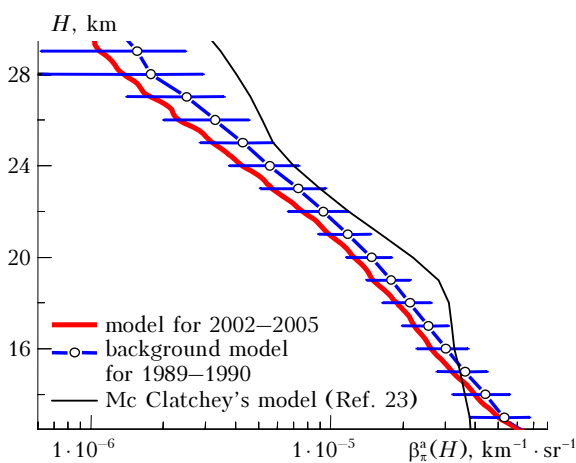


Fig. 4. Models of altitude distribution of aerosol backscattering coefficient at $\lambda = 532$ nm. The horizontal lines show standard error corridor for the model of 1989–1990 period.

It is seen that, above 17 km, the statistical model²³ overestimates our empirical values and demonstrates more complex stratification, with a pronounced inflection point at altitudes of 18–20 km, characterizing the Junge layer, i.e., the residual volcanic aerosol. For background 1989–1990 and 2002–2005 models, the Junge layer is not so evident, that says about its volcanic origin. Comparison of our empirical 1989–1990 and 2002–2005 models shows that under conditions of long-term VQP the B_{π}^a values are lower throughout the altitude range, and that a more intense aerosol removal from stratosphere in SAL levels above 20 km took place.

3. Discussion of results and conclusions

Based on statistical analysis of results of SA sensing in 1986–2003, earlier we revealed¹⁹ a quasi-biennial oscillation (QBO) in time behavior of integrated aerosol backscattering coefficient for stratosphere over Tomsk and indicated its correlation with QBO stratospheric general circulation. The latter is determined by alternation of periods of predominate easterly and westerly zonal winds in the equatorial stratosphere (easterly and westerly QBO phases). Moreover, in the westerly QBO phase, when the meridional transport from tropical belt to middle and high latitudes increases,²² the SA growth and maximum SA abundances are observed in Tomsk. An opposite pattern is observed in the easterly QBO phase, when the meridional transport decays. The QBO effects hold both under conditions of volcanically perturbed stratosphere and in periods of background SAL state. All this argues for hypothesis of existence of tropical reservoir both of volcanic and background stratospheric aerosol.^{16,19,20} This reservoir is an additional aerosol source for the stratosphere of middle and high latitudes.

The presence of tropical reservoir of background SA is under debate for a long time. Data of investigations under conditions of long-term volcanically quiet period support this hypothesis to a considerable degree. The last models of background sulfate aerosols, developed on the base of atmospheric general circulation models with inclusion of chemical processes, show^{7,8} that the formation of new SA particles through homogeneous nucleation takes place predominately in the tropical lower stratosphere. The main sulfur-containing source for formation of $(\text{H}_2\text{SO}_4 : \text{H}_2\text{O})$ SA particles is SO_2 and OCS surface emission.⁸ Although the surface emission of SA gas precursors in Northern Hemisphere midlatitudes is higher than at equator, the convection from troposphere to stratosphere in tropical belt is higher than in midlatitudes, which leads to formation of the background SA tropical reservoir. Its presence is also confirmed by data of lidar observations at middle^{17,20} and tropical latitudes,²⁸ as well as by SAGE data.^{22,24,25} The seasonal and quasi-biennial variations of vertical distribution and integrated SA content at

observation points are related to corresponding changes of general troposphere–stratosphere circulation (TSC). General TSC models suggest^{29–31} that the tropical tropopause is the main region of tropospheric air entry into stratosphere, where the meridional transport of air masses to the middle and high latitudes takes place with subsequent sinking to troposphere. This process is most pronounced within the circumpolar vortex and shows seasonal variations with a winter maximum.³¹ The study of the processes of stratosphere–troposphere exchange in more detail is now carried out at the Siberian Lidar Station, which will be the subject of our future publications.

Based on long-term lidar observations, we developed empirical models of vertical distribution of the optical characteristics of midlatitude background stratospheric aerosol under conditions of long-term volcanically quiet period. Measurement data on seasonal and quasibiennial variations of stratospheric aerosol loading at a single midlatitude observation point reflect the processes of stratospheric general circulation through the influence of the aerosol meridional transport from the tropical reservoir.

Acknowledgments

This work was performed at the Siberian Lidar Station (reg. No. 01-64) under support of Federal Agency of Science and Innovations, as well as Russian Foundation for Basic Research (Grant No. 05-05-64518), and International Scientific Technical Center (Project No. B-1063).

References

1. P.B. Russel, J.M. Livingston, R.F. Pueschel, J.J. Bauman, J.B. Pollack, S.L. Brooks, P. Hamill, L.W. Thomason, Stowe L.L., T. Deshler, E.G. Dutton, and R.W. Bergstrom. *J. Geophys. Res. D* **101**, No. 13, 18.745–18.763 (1996).
2. A. Lacis, J. Hansen, and M. Sato, *Geophys. Res. Lett.* **19**, No. 15, 1607–1610 (1992).
3. M. Sato, J.E. Hansen, M.P. McCormick, and J.B. Pollack, *J. Geophys. Res. D* **98**, No. 12, 22.987–22.994 (1993).
4. M.P. McCormick, L.W. Thomason, and C.R. Trepte, *Nature, (Gr. Brit.)* **373**, 399–404 (1995).
5. K. Labitzke and M.P. McCormick, *Geophys. Res. Lett.* **19**, No. 2, 207–210 (1992).
6. H. Jager and F. Homburg, in: *Abstracts of Papers at 19th ILRC*. Langley Research Center, Hampton, Virginia (1998), pp. 335–338.
7. C. Timmreck, *J. Geophys. Res. D* **106**, No. 22, 28313–28332 (2001).
8. M. Takigawa, M. Takahashi, and H. Akiyoshi, *J. Geophys. Res. D* **107**, No. 22, AAC1/1–AAC1/11 (2002).
9. V.V. Zuev, A.V. El'nikov, and V.D. Burlakov, *Atmos. Oceanic Opt.* **12**, No. 3, 257–264 (1999).
10. V.V. Zuev, V.D. Burlakov, and A.V. El'nikov, *J. Aerosol Sci.* **29**, No. 10, 1179–1187 (1998).
11. V.V. Zuev, V.D. Burlakov, A.V. El'nikov, A.P. Ivanov, A.P. Chaikovskii, and V.N. Shcherbakov, *Atmos. Environ.* **35**, 5059–5066 (2001).
12. V.V. Zuev, V.E. Zuev, V.D. Burlakov, S.I. Dolgii, A.V. Elnikov, A.V. Nevzorov, and V.L. Pravdin, *Atmos. Oceanic Opt.* **16**, No. 2, 111–115 (2003).
13. V.V. Zuev, V.E. Zuev, V.D. Burlakov, S.I. Dolgii, A.V. El'nikov, and A.V. Nevzorov, *Atmos. Oceanic Opt.* **16**, No. 8, 663–667 (2003).
14. V.D. Burlakov, S.I. Dolgii, and A.V. Nevzorov, *Atmos. Oceanic Opt.* **17**, No. 10, 756–762 (2004).
15. V.V. Zuev, A.V. Elnikov, and V.D. Burlakov, *Laser Sensing of the Middle Atmosphere*, ed. by V.V. Zuev (RASKO, Tomsk, 2002), 352 pp.
16. G.S. Kent and G.M. Hansen, *Appl. Opt.* **37**, No. 18, 3861–3872 (1998).
17. D.S. Woods, M.T. Osborn, and P.L. Lucker, *Proc. SPIE* **4882**, 474–480 (2002).
18. T. Deshler, M.E. Hervig, D.J. Hofmann, J.M. Rosen, and J.B. Liley, *J. Geophys. Res. D* **108**, No. 5, 4/1–4/13 (2003).
19. V.V. Zuev, A.V. El'nikov, and V.D. Burlakov, *Atmos. Oceanic Opt.* **17**, No. 12, 880–884 (2004).
20. H. Jager, in: *Reviewed and Revised Papers Presented at the 22nd International Laser Radar Conference* (Matera, Italy, 2004), Vol. 2, pp. 563–566.
21. V.V. Zuev, V.D. Burlakov, A.V. El'nikov, S.V. Smirnov, and P.A. Khryapov, *Atmos. Oceanic Opt.* **13**, No. 11, 930–935 (2000).
22. M.H. Hitchman, M. McKay, and C.R. Trepte, *J. Geophys. Res. D* **99**, No. 10, 20689–20700 (1994).
23. R.A. McClatchey, R.W. Fenn, J.E.A. Selby, et al., *Optical Properties of the Atmosphere* (revised). Report AFCRL-71-0279, AFCRL (Bedford, 1971), 98 pp.
24. C.R. Trepte, L.W. Thomason, and G.S. Kent, *Geophys. Res. Lett.* **21**, No. 22, 2397–2400 (1994).
25. G.S. Kent, C.R. Trepte, and P.L. Lucker, *J. Geophys. Res. D* **103**, No. 22, 28863–28874 (1998).
26. D.J. Hofmann, *Science* **248**, 996–1000 (1990).
27. M.L. Asaturov, *Meteorol. Gidrol.*, No. 3, 5–12 (1998).
28. J.E. Barnes and D.J. Hofmann, *Geophys. Res. Lett.* **28**, No. 15, 2895–2898 (2001).
29. A.E. Dessler, E.J. Hintsa, E.M. Weinstock, J.G. Anderson, and K.R. Chan, *J. Geophys. Res.* **100**, No. 11, 23167–23172 (1995).
30. P. Hoor, H. Fischer, L. Lange, J. Lelieveld, *J. Geophys. Res. D* **107**, No. 5, ACL1/1–ACL1/11 (2002).
31. C. Appenzeller, J.R. Holton, and K.H. Rosenlof, *J. Geophys. Res.* **101**, No. 7, 15071–15078 (1996).